Chapter 9
Chemoelectrical Gas Sensors of Metal Oxides with and Without Metal Catalysts

G. A. Mousdis, M. Kompitsas, G. Petropoulou, and P. Koralli

Abstract The interest for gas sensors is uprising due to the increased demand for many applications such as: Security, Environment, Industry, Medicine etc. Therefore, the development of new, cheap, easy to prepare, simple, low energy consuming and reliable sensors have become of great significance. A category of gas sensors with these characteristics is the metal oxide chemoelectrical sensors that are the most common ones used today. The sensing properties of these sensors depend mainly on the surface properties such as roughness, porosity, crystallinity etc. that are strongly depended on the preparation method. Moreover, the addition of metal nanoparticles and especially nanoparticles of noble metals with catalytic properties differentiate (mostly improve) the sensing efficiency. In this work we used the PLD technique to prepare thin films of Cu_xO ($1 < x < 2$) and surface decorated some of them with gold nanoparticles to be used as sensors. These sensors consisted of the sensing thin film on the surface of a quartz tube surrounding a ceramic heater with low thermal capacity. The films are characterized by AFM and SEM techniques. A significant response to several concentrations of the hydrogen and acetone at relative low temperatures was demonstrated.

Keywords Cu_xO thin films · Au · Nanoparticles · Hydrogen sensor · Acetone sensor

9.1 Introduction

Gas sensors have a great impact on many areas such as security, environment, industry, medicine, automotive applications, space houses, sensors networks etc. Moreover, process and manufacturing industries find extensive applications of

G. A. Mousdis (✉) · M. Kompitsas · G. Petropoulou · P. Koralli
NHRF-National Hellenic Research Foundation, Theoretical and Physical Chemistry Institute-TPCI, Athens, Greece
e-mail: gmousdis@eie.gr

J. Bonča, S. Kruchinin (eds.), *Advanced Nanomaterials for Detection of CBRN*,
NATO Science for Peace and Security Series A: Chemistry and Biology,
https://doi.org/10.1007/978-94-024-2030-2_9

various toxic and combustible gases, such as hydrogen sulfide (H_2S) [1], NH_3 [2] CO [3], H_2 [4], flammable volatile organic compounds [5] etc. Gas sensors can monitor the concentration of these gases detecting and avoiding gas leaks.

There is a huge need in the market for new cheap small, stable reliable and low power consuming gas sensors. This need in combination with the large applications range triggered the last decades a huge worldwide research for new sensor materials with improved properties. Gas sensor manufacturing technologies have been further improved by the development of nanotechnology [6–10], low-power and low-cost microelectronic circuits [11], chemometrics [12, 13], and microcomputing [14, 15]. The global gas sensor market was valued at USD 2.05 billion in 2018 and an increase of 7.8% from 2019 to 2025 is expected (http://www.grandviewresearch.com/industry-analysis/gas-sensors-market).

A gas sensor is a transducer that converts the presence and measures the concentration of a gas into a physical property [16]. There are many categories of gas sensors such as electrochemical, optical, semiconducting, capacitance, calorimetric, ultrasonic etc. The type of sensor to be used depends on the application demands and characteristics. The factors that have great importance in the sensor type decision are: gas type and concentration range, humidity, temperature, pressure, gas velocity, chemical poisons and/or interfering species, power consumption, response time, maintenance interval, fixed or portable, point or open path etc.

The most common category of gas sensors are the resistivity sensors (also known as chemiresistors). The transduction mechanism of resistive gas sensors is based on the change in resistance of the sensing layer upon adsorption and reaction with the target gas molecules. The sensing layer usually determines the sensitivity and the selectivity. In most cases, the sensing material is an organic polymer [17, 18], an organic [19] or hybrid semiconductor [20] or a metal oxide (MO_x) [21]. Although the number of chemiresistors based on polymers is increasing [22], those based on metal oxides are the most popular. Their popularity is due to: simple construction, low cost, compact size, high compatibility with microelectronic processing high accuracy, big variety of detectable gases, and their ability to monitor on a real-time basis. Gas-sensing characteristics such as gas response, selectivity, stability, and short response/recovery time are closely dependent upon the preparation method and condition of the sensor. But there are two main disadvantages, their poor selectivity and the elevated operating temperatures. The addition of a catalyst can decrease the operating temperature and even increase the selectivity and the sensitivity in respect to a specific analyte gas.

The MO_x films can detect, reductive (e.g., H_2, CO, Hydrocarbons), oxidative (e.g., O_2, O_3) or neutral (e.g., CO_2, H_2O) gases. Their main use is the detection of leaks of toxic or explosive gases at chemical and industrial processes [23]. Lately their use is expanded into many other activities concerning human health [24], drinks and food quality monitoring [25], traffic safety [26] etc. A big variety of transition or post transition metals have been used for the preparation of metal oxide sensors. The main reason of choosing these metals is the small energy difference of their cations (d^n configuration) with the d^{n+1} or d^{n-1} configuration [14]. The most

effective metal oxide sensors are those with cation configurations d^0 (e.g. TiO_2) or d^{10} (e.g. SnO_2, ZnO).

Copper is a transition metal with the Cu^+ and Cu^{+2} configuration [Ar]-$3d^{10}$, -d^9 respectively. The difference in energy between these two states is small because of the primarily antibonding character of these two high-lying d orbitals [27]. Copper oxide (CuO) is a p-type semiconductor with a direct bandgap of 1.2–1.9 eV [28]. Gas sensors based on CuO nanostructures have attracted considerable attention because of their excellent sensitivity and selectivity in detecting a range of gases and vapors: water vapor, HCOH, C_2H_5OH, NO_2, H_2S, and CO [29, 30]. A range of different techniques such as wet chemical methods [31], sol-gel [32], spray pyrolysis [33], sputtering [34] etc. have been used to prepare CuO thin films.

As a part of research to understand and configure the parameters that influence the sensing properties of MO_x films, we have prepared copper oxide thin films with and without dispersed gold nanoparticles on quartz tubes substrates using the Pulsed Laser Deposition technique (PLD). The thin films were studied as gas sensors and the effect of the Au nanoparticles as a catalyst on gas sensing was investigated. Structural, morphological, and compositional properties were studied by atomic force microscopy (AFM), Scanning Electron Microscopy (SEM), and Energy Dispersive X-ray (EDS) Spectroscopy, respectively. The sensing properties of CuO and CuO:Au towards H_2, and acetone were investigated at different concentrations and operating temperatures up to 345 °C.

9.2 Experimental Techniques

9.2.1 Film Growth

The CuO thin film sensor has been grown by the PLD method (Fig. 9.1a) [35, 36]. The laser beam was delivered by a Mo. Nano S 130-10 Q-switched Nd:YAG laser (Litron Lasers) 532 nm and with pulse duration 10 ns. The repetition rate was 10 Hz and a total of 4 h was employed to complete a deposition. The beam was focused on the Cu target resulting to 14 J/cm^2 fluence. This foil target was mounted on a XY-translation stage that was driven by a microprocessor and performed a meander-like movement. Thus, target drilling was avoided. Before deposition, the high vacuum chamber was pre-evacuated down to a base pressure of 10^{-5} mbar. Then, oxygen reactive gas was inserted and kept at a 20 Pa dynamic pressure during film growth. The CuO thin film was deposited under RT on a Pyrex tube substrate ($D_{in} = 8$ mm, thickness 1 mm) that was rotating vertically by an electrical motor with a few revolutions/s. After deposition, the CuO thin film was annealed at 500 °C for 1 h. For the CuO:Au compound thin film sensor, a gold target was ablated for 15 min in vacuum by the same technique as above to partially cover the CuO thin film surface with Au nanoparticles and all measurements were repeated.

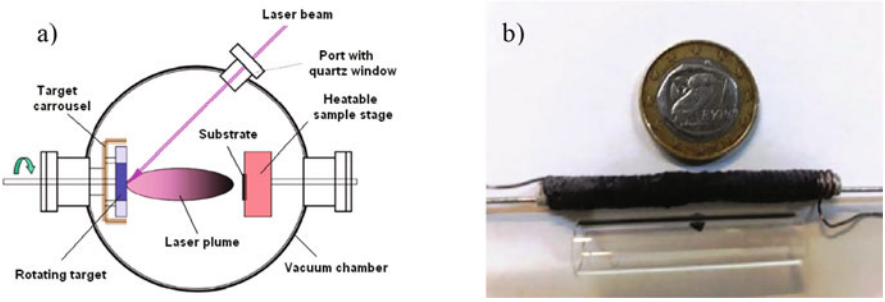

Fig. 9.1 (**a**) Schematic diagram of the PLD set-up for the preparation of Cu_xO and Cu_xO–Au doped films. (**b**) Photo of the high temperature ceramic cylindrical heater and the CuO thin film on a quartz tube

9.2.2 Gas Testing Apparatus

Gas testing was performed inside an aluminum chamber with controllable pressure. For sensing, the tube substrate was heated by a home-made cylindrical oven: this consisted of an alumina tube (4 mm in Dia.) including a Ni–Ni/Cr thermocouple for temperature measurement, a Ni–Cr wire wrapping up the tube that served as heating element (Fig. 9.1b) with the current from a stabilized power supply to set the desired operating temperature. A high-temperature paste covered the oven and transferred the heat to the quartz tube substrate efficiently. Prior to gas testing, the chamber was evacuated down to 10^{-4} mbar by a mechanical pump. Then the chamber was filled with atmospheric pressure from a bottle (80% N_2, 20% O_2), by using a Bronkhorst gas flowmeter and the pressure was controlled by a Baratron gauge. Analyte gas concentrations were calculated from partial pressure measurements displayed on the Baratron gauge. The film sensor was connected in series with a Keithley pico-Ameter in an electrical circuit, biased by a voltage of $1\,V_{dc}$. Upon inserting the analyte gas, the resistivity change of the sensor resulted to a current change through the circuit that was recorded in real time, digitized and displayed on the computer screen.

9.3 Films Characterization

9.3.1 Scanning Electron Microscopy (SEM/EDS) Results

Figure 9.2 show SEM images of the prepared CuO films with different magnification. As we can observe (Fig. 9.2a), a smooth and uniform surface of CuO film is formed with small particles (size $<5\,\mu m$) on it. It is known from the literature that PLD grown thin films exhibit on their surface a large number of such droplet-like

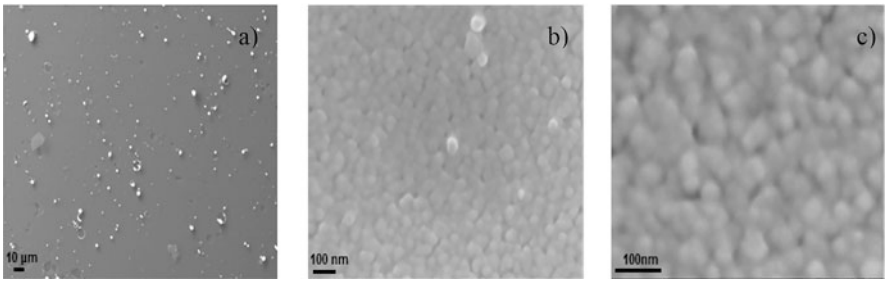

Fig. 9.2 SEM images of CuO film

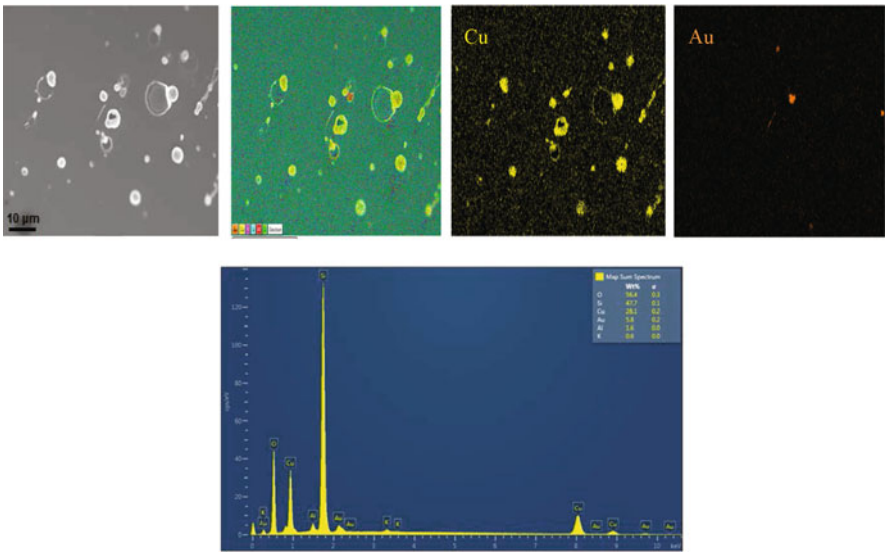

Fig. 9.3 SEM and EDS images of CuO:Au film

particles that consist of pure target material (here copper) which is ejected from the target during laser ablation. Images of higher magnification (Fig. 9.2b and c) reveal that the surface of CuO is granular, highly dense and compact, consisting of a homogeneous distribution of CuO grains with sizes 50–80 nm.

The SEM/EDS analysis (Fig. 9.3) confirmed that the droplet-like particles consist indeed of Cu (the yellow colour corresponds to Cu). Moreover, we can see on the surface of the CuO/Au films small particles of Au with sizes ~1 µm (orange colour is the Au).

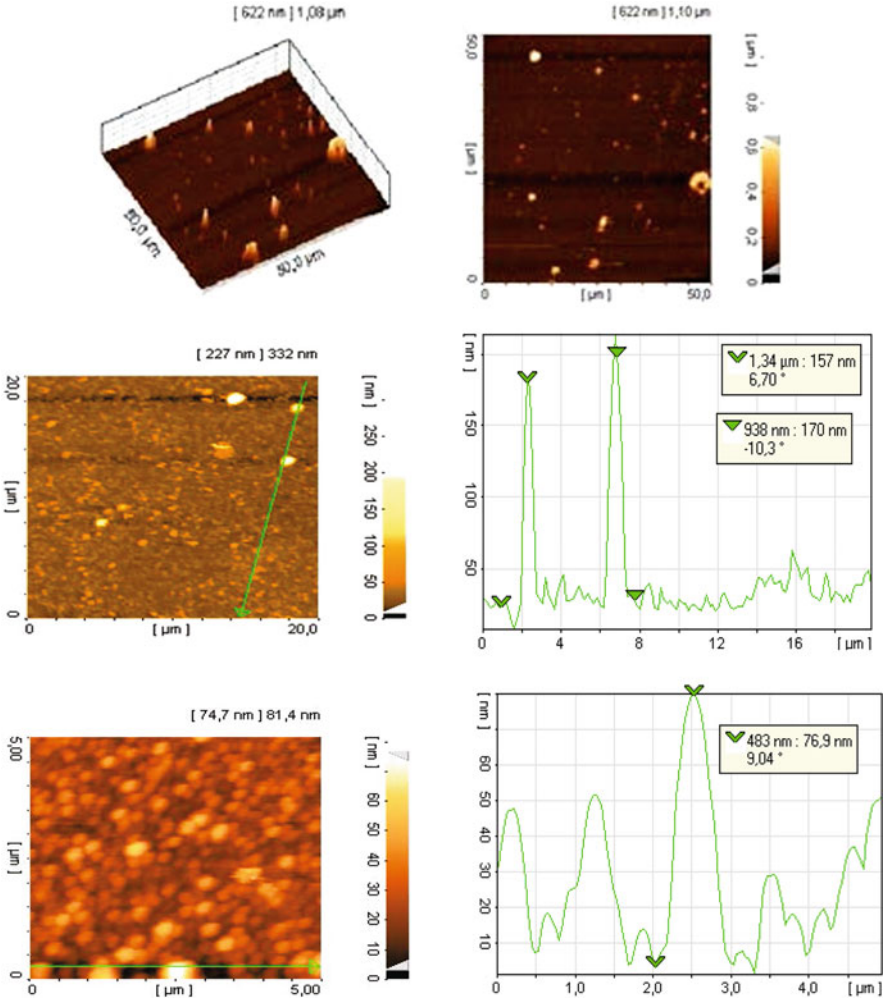

Fig. 9.4 3D, 2D and profile AFM images of CuO films

9.3.2 Atomic Force Microscopy (AFM) Results

From the AFM images (Fig. 9.4) we can see that the surface of the films is uniform with some Cu particles on it with sizes heights less than 700 nm. From the two-dimensional AFM (contact mode) images, as well as from the profile images, we observe that the surface of the films is very smooth and exhibit hillock morphology, including columnar grains growing along the c-axis, perpendicular to the substrate surface. The grain boundaries of CuO are clear and the grains seem to have similar dimensions and round shape in plane.

9.4 Gas Sensing Results

9.4.1 Sensing Mechanism

The fundamental sensing mechanism of metal oxide based gas sensors relies on the change in electrical resistivity of thin films on exposure to a target gas. The gas molecules interact with the metal oxide surface, acting as donors or acceptors of electrons thus altering the resistivity of the metal oxide film. Initially, O_2 air molecules are adsorbed on the film surface, bind to it by film electrons, and subsequently dissociates and transforms to charged ions according to the following reactions:

$$O_2\ (\text{gas-adsorb}) + e^- \longleftrightarrow O_2^-\ (T \leqslant 200\,^\circ C)$$

$$1/2O_2\ (\text{gas-adsorb}) + e^- \longleftrightarrow O^-\ (T \geqslant 200\,^\circ C)$$

$$1/2O_2\ (\text{gas-adsorb}) + 2e^- \longleftrightarrow O^{-2}\ (T \geqslant 200\,^\circ C)$$

The reactions are endothermic and the equilibrium is moved to the right by increasing the temperature [37]. The gas molecules to be detected react with the adsorbed oxygen are oxidized and as a result the bonding electron is released back to the film. This induces a change of the number of charge carriers of the semiconducting metal oxide and consequently its resistivity (Fig. 9.5). Depending of the semiconductor type (n- or p-type) of the sensor and the type of analyte gas (oxidizing or reducing) the resistivity increases or decreases respectively [38] (Table 9.1).

Besides the type of the analyte, the magnitude of the resistivity change for a specific MO_x film to an analyte depends on the number of the surface complexes, the proximity to the gas, and the sensor temperature. For these reasons the morphology of the sensing layer (e.g. porosity, crystallinity, and surface roughness etc.) are

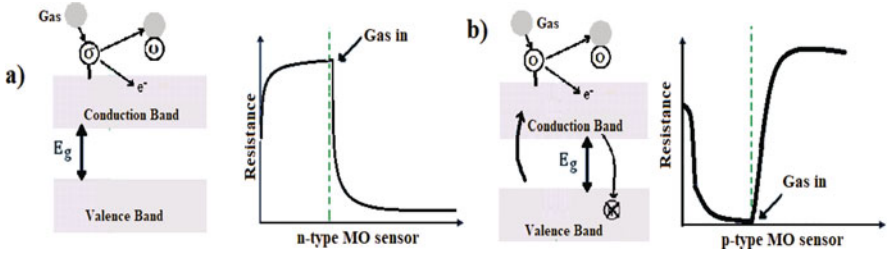

Fig. 9.5 Schematic representation of band models of conductive mechanism and resistance change for (**a**) an n- or (**b**) p-type metal oxide, without and with exposure to analyte gas, for reducing gases

Table 9.1 Dependence of resistance change from the type of semiconductor and the gas

Classification	Oxidizing gases	Reducing gases
n-type	Resistance increase	Resistance decrease
p-type	Resistance decrease	Resistance increase

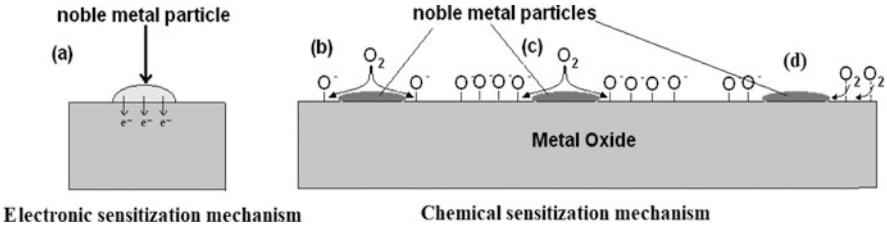

Fig. 9.6 Schematic depiction of the electronic sensitization mechanism (**a**) and the chemical sensitization mechanism (**b**, **c**, **d**)

crucial for the sensor efficiency [39]. As a consequence, the properties of the sensor strongly depend on the preparation method and processing (e.g. annealing).

The sensing properties can be improved by the presence of metal nanoparticles (mostly noble metals) on the surface of the sensor. This improvement can be attributed to two different sensitization mechanisms: (a) the electronic sensitization, caused by interfacial electronic redistribution and (b) the chemical sensitization [40]. In the electronic sensitization mechanism, there is a transfer of electrons between the noble metal and the MO_x beneath, due to the work function difference (Fig. 9.6a). In the chemical sensitization mechanism, the noble metals facilitate the chemical reactions between target gas and metal oxide surface through the spill-over phenomenon [4, 41]. The results depend strongly on the type and the concentration of the noble metal.

More specifically, the action of noble metal nanoparticles is based manly in the production of charged oxygen species due to highly effective dissociation catalytic ability (Fig. 9.6b) [42]. The noble metals are effective oxygen dissociation catalysts. They react with oxygen molecules and dissociate them to charged species (Fig. 9.6b). The charged oxygen diffuses onto the surface of the metal oxide (Fig. 9.6c). In addition, the noble metal nanoparticles attract and dissociate the O_2 molecules adsorbed in the neighboring metal oxide area before desorption (Fig. 9.6d). As a result, they create an "effective area" [43] around the metal nanoparticle with an increased number of charged species. Therefore, the ideal case would be that the nanoparticles are evenly dispersed on the surface so that these "effective areas" cover the whole surface of the film.

In many cases the nanoparticles also catalyze the reaction of the analyte with the O species e.g. in the case of H_2 the following reactions occur:

$$\text{(a) } H_2(g) \rightarrow 2H_{ads}, \quad \text{(b) } H_{ads} \rightarrow H^+_{ads} + e^-,$$
$$\text{(c) } H^+_{ads} + O^-_{ads} \rightarrow OH, \quad \text{(d) } 2OH \rightarrow H_2O + O_{ads},$$

where the first 2 reactions (a and b) were catalyzed by Pd.

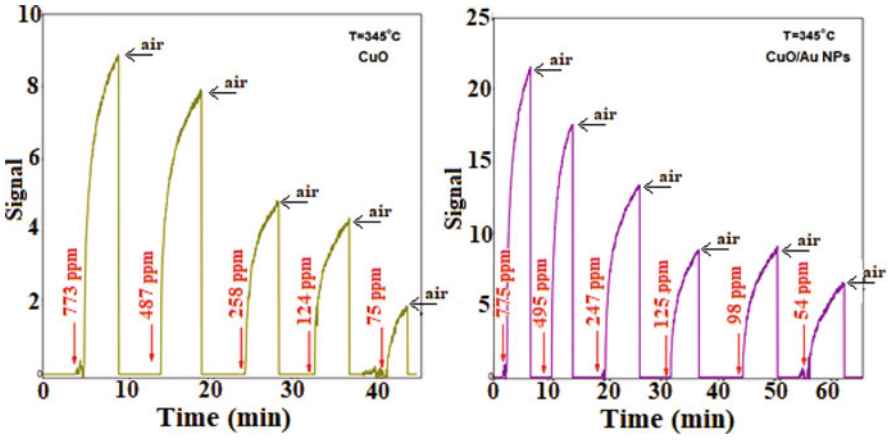

Fig. 9.7 Response of the CuO and CuO:Au sensors at 345 °C for different concentrations of H_2

9.4.2 H_2 Sensing

Hydrogen sensing was studied at two different temperatures (305 °C and 345 °C). In all cases there was a clear and fast response to the presence of H_2 (rise time less than 1 min). A typical set of real-time measurements is shown in Fig. 9.7 which presents the transient response of a CuO and a CuO:Au sensor to various concentrations of H_2 in air, for an operating temperature of 345 °C.

In the case of the Au doped sample the signal at 305 °C was more than three times bigger than that of the pure CuO (Fig. 9.8) resulting at a lower detection limit (Table 9.2). By increasing the temperature the signal improved significantly in the case of pure CuO and slightly in the case of CuO:Au sensor.

The enhancement of the sensor sensitivity towards hydrogen has been also observed previously in the case of the NiO:Au nanocomposites [44]. Au nanoparticles acting as catalysts are reducing the dissociation barrier for both hydrogen and atmospheric oxygen in their vicinity. The produced highly active atomic species interact with each other very fast, in particular at this high operating temperature, and it results to an additional increase of the film resistance [45].

9.4.3 Acetone Sensing

Acetone sensing was studied at two different temperatures (305 °C and 340 °C). In both cases, we can observe again a clear and fast response to the presence of acetone. A typical set of real-time measurements is shown in Fig. 9.9, which presents the transient response of a CuO and a CuO:Au sensor to various concentrations of acetone in air, for an operating temperature of 340 °C. On Fig. 9.10 we can see

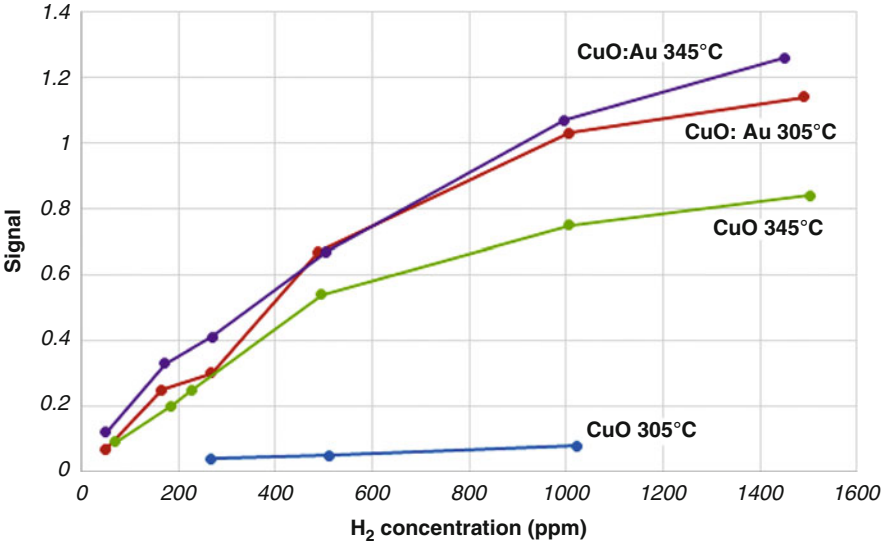

Fig. 9.8 Diagrams of the CuO and CuO:Au sensors response at 305 °C and 345 °C for different concentrations of H_2

Table 9.2 Detection Limits of CuO and CuO: Au sensors at 305 °C and 345 °C

Sample		Lower detection limit of H_2	Lower detection limit of acetone
CuO	At 305 °C	267 ppm	56 ppm
CuO:Au		50 ppm	128 ppm
CuO	At 345 °C	70 ppm	7 ppm
CuO:Au		50 ppm	12 ppm

the response of CuO and CuO:Au sensors to various concentrations of Acetone in air at 305 °C and 345 °C.

We can notice from this graph that partial surface coverage with Au particles deteriorates the sensor sensitivity towards acetone at both temperatures, in contrast with what was observed in the case of H_2. A possible explanation would be as follows: Au metallic nanoparticles act as catalysts again, promoting the dissociation of adsorbed oxygen only, but not the dissociation of acetone that would lead to signal enhancement, as for H_2. On the other side, the Au nanoparticles cover a part of the film surface, therefore less film surface is available to acetone to oxidize. To prove this hypothesis, more CuO:Au nano-composites with different concentrations of Au nanoparticles are necessary to be tested as acetone sensors. Such experiments are now under consideration.

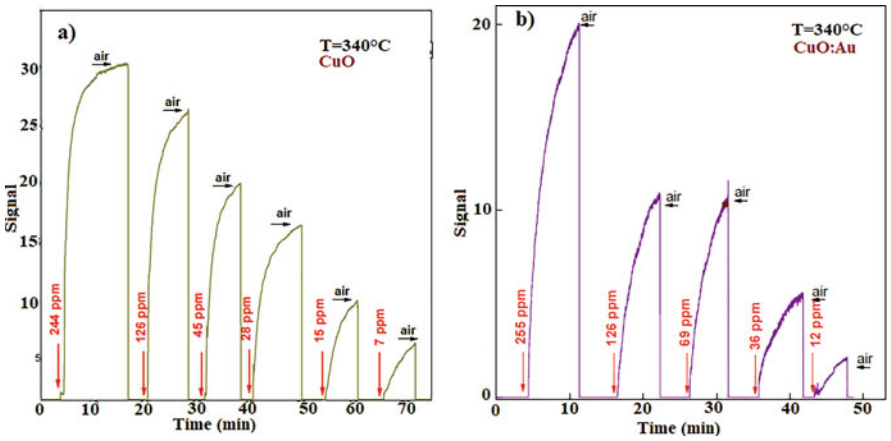

Fig. 9.9 Response of the CuO and CuO:Au sensors at 340 °C for different concentrations of Acetone

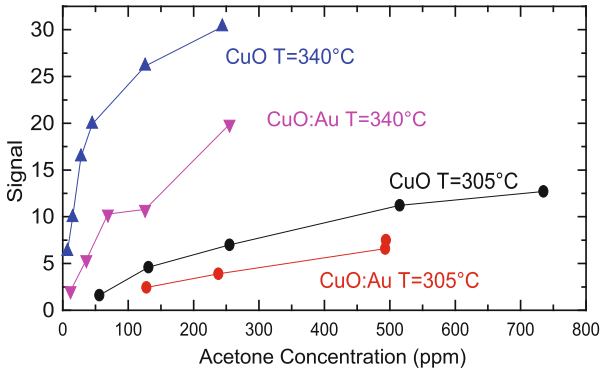

Fig. 9.10 Diagrams of the CuO and CuO:Au sensors response at 305 °C and 340 °C for different concentrations of Acetone

9.5 Conclusions

We have deposited CuO and nanocomposite CuO:Au thin films on quartz tubes by the PLD technique. A new type high temperature ceramic cylindrical heater was inserted into the tubes to prepare low cost gas sensors. AFM and SEM/ADX images have shown the granular film surface with a large effectiveness, appropriate to be used as gas sensors. They were tested as H_2 and acetone sensors with satisfactory results. The presence of Au nanoparticles on the film surface enhances in the case of H_2 detection the sensing efficiency significantly, but in the case of acetone deteriorates it. The experimental results showed that CuO and CuO:Au films prepared by PLD can be used as cost effective sensors. Experiments are in progress

towards lower concentrations of the analytes, and investigating parameters such as the concentration and the type of noble metals.

Acknowledgments We acknowledge support of this work by the project "Advanced Materials and Devices" (MIS 5002409) which is implemented under the "Action for the Strategic Development on the Research and Technological Sector", funded by the Operational Program "Competitiveness, Entrepreneurship and Innovation" (NSRF 2014–2020) and co-financed by Greece and the European Union (European Regional Development Fund). One of the authors (P. Koralli) would like to thank the "IKY Fellowships of Excellence for Postgraduate Studies in Greece – SIEMENS PROGRAM" for a scholarship.

References

1. Gong J, Chen Q, Lian M-R, Liu N-C, Stevenson RG, Adami F (2006) Micromachined nanocrystalline silver doped SnO_2 H_2S sensor. Sens Actuators B Chem 114:32
2. Aspiotis N, El Sachat A, Athanasekos L, Vasileiadis M, Mousdis G, Vainos N, Riziotis C (2013) Diffractive ammonia sensors based on Sol–Gel nanocomposites materials. Sens Lett 11:1415
3. Stamataki M, Mylonas D, Tsamakis D, Kompitsas M, Tsakiridis P, Christoforou E (2013) CO-sensing properties of Cu_xO-based nanostructured thin films grown by reactive pulsed laser deposition. Sens Lett 11:1964
4. Fasaki I, Suchea M, Mousdis G, Kiriakidis G, Kompitsas M (2009) The effect of Au and Pt nanoclusters on the structural and hydrogen sensing properties of SnO_2 thin films. Thin Solid Films 518:1109
5. Alexiadou M, Kandyla M, Mousdis M, Kompitsas M (2017) Pulsed laser deposition of ZnO thin films decorated with Au and Pd nanoparticles with enhanced acetone sensing performance. Appl Phys A 123:262
6. Lima T-C, Ramakrishna S (2006) A conceptual review of nanosensors. Z Naturforsch 61a:402
7. Ermakov V, Kruchinin S, Fujiwara A (2008) Electronic nanosensors based on nanotransistor with bistability behaviour. In: Bonca J, Kruchinin S (eds) Proceedings NATO ARW "Electron transport in nanosystems". Springer, pp 341–349
8. Ermakov V, Kruchinin S, Hori H, Fujiwara A (2007) Phenomena in the resonant tunneling through degenarate energy state with electron correlation. Int J Mod Phys B 11:827–835
9. Ermakov V, Kruchinin S, Pruschke T, Freericks J (2015) Thermoelectricity in tunneling nanostructure. Phys Rev B 92:115531
10. Repetsky SP, Vyshyvana IG, Nakazawa Y, Kruchinin SP, Bellucci S (2019) Electron transport in carbon nanotubes with adsorbed chromium impurities. Materials 12:524
11. Chiu S-W, Tang K-T (2013) Towards a chemiresistive sensor-integrated electronic nose: a review. Sensors 13:14214
12. Lavine B, Workman J (2008) Chemometrics. Anal Chem 80:4519
13. Pravdova V, Pravda M, Guilbault GG (2007) Role of chemometrics for electrochemical sensors. Anal Lett 35:2389
14. Hagleitner C, Hierlemann A, Lange D, Kummer A, Kerness N, Brand O, Baltes H (2001) Smart single-chip gas sensor microsystem. Nature 414:293
15. Feng S, Farha F, Li Q, Wan Y, Xu Y, Zhang T, Ning H (2019) Review on smart gas sensing technology. Sensors (Basel, Switzerland) 19:3760
16. Mousdis G, Kompitsas M, Fasaki I (2011) Electrochemical sensors for the detection of hydrogen prepared by pld and sol-gel chemistry. In: Reithmaier JP, Paunovic P, Kulisch W, Popov C, Petkov P (eds) Proceedings NATO ARW "Nanotechnological basis for advanced sensors". Springer, pp 401–407

17. Indarit N, Kim Y-H, Petchsang N, Jaisutti R (2019) Highly sensitive polyaniline-coated fiber gas sensors for real-time monitoring of ammonia gas. RSC Adv 46:26773
18. Cichosz S, Masek A, Zaborski M (2018) Polymer-based sensors: a review. Polym Test 67:342
19. Garcia-Breijo E, Gómez-Lor Pérez B, Cosseddu P (eds) (2016) Organic sensors: materials and applications. Institution of Electrical Engineers, India, SciTech Publishing, Inc. ISBN: 978-1-84919-985-8
20. Wang S, Kang Y, Wang L, Zhang H, Wang Y (2013) Organic/inorganic hybrid sensors: a review. Sens Actuators B Chem 182:467
21. Adhikari B, Majumdar S (2004) Polymers in sensor applications. Prog Polym Sci 29:699
22. Lee J-H (2019) Technological realization of semiconducting metal oxide-based gas sensors. In: Barsan N, Schierbaum K (eds) Metal oxides, gas sensors based on conducting metal oxides. Elsevier, Amsterdam/Oxford/Cambridge, p 167–216, ISBN: 9780128112243
23. Oyabu T (1991) A simple type of fire and gas leak prevention system using tin oxide gas sensors. Sens Actuators B 5:221
24. Xing R, Xu L, Song J, Zhou C, Li Q, Liu D, Wei Song H (2015) Preparation and gas sensing properties of In_2O_3/Au nanorods for detection of volatile organic compounds in exhaled breath. Sci Rep 5:10717
25. Ghasemi-Varnamkhasti M, Mohtasebi SS, Siadat M, Lozano J, Ahmadi H, Razavi SH, Dicko A (2011) Aging fingerprint characterization of beer using electronic nose. Sens Actuators B 159:51
26. Seetha M, Mangalaraj D (2012) Nano-porous indium oxide transistor sensor for the detection of ethanol vapours at room temperature. Appl Phys A 106:137
27. Schneider WF, Hass KC, Ramprasad R, Adams JB (1996) Cluster models of Cu binding and CO and NO adsorption in Cu-exchanged zeolites. J Phys Chem 100:6032
28. Comini E, Faglia G, Sberveglieri G, Pan Z, Wang ZL (2002) Stable and highly sensitive gas sensors based on semiconducting oxide nanobelts. Appl Phys Lett 81:1869
29. Stamataki M, Mylonas D, Tsamakis D, Kompitsas M, Tsakiridis P, Christoforou E (2013) CO-sensing properties of Cu_xO-based nanostructured thin films grown by reactive pulsed laser deposition. Sens Lett 11:1964
30. Liao L, Zhang Z, Yan B, Zheng Z, Bao QL, Wu T, Li CM, Shen ZX, Zhang JX, Gong H (2009) Multifunctional CuO nanowire devices: P-type field effect transistors and CO gas sensors. Nanotechnology 20:085203
31. Wang W, Liu Z, Liu Y, Xu C, Zheng CC, Wang G (2003) A simple wet-chemical synthesis and characterization of CuO nanorods. Appl Phys A 76:417
32. Armelao L, Barreca D, Bertapelle M, Bottaro G, Sada C, Tondello E (2003) A sol-gel approach to nanophasic copper oxide thin films. Thin Solid Films 442:48
33. Moumen A, Hartiti B, Comini E, El Khalidi Z, Arachchige HMMM, Fadili S, Thevenin P (2019) Preparation and characterization of nanostructured CuO thin films using spray pyrolysis technique. Superlattice Microstruct 127:2
34. Samarasekara P, Kumara NTRN, Yapa NUS (2006) Sputtered copper oxide (CuO) thin films forgas sensor devices. J Phys Condens Matter 18:2417
35. Fasaki I, Giannoudakos A, Stamataki M, Kompitsas M, Gyorgy E, Mihailescu IN, Roubani-Kalantzopoulou F, Lagoyannis A, Harissopulos S (2008) Nickel oxide thin films synthesized by reactive pulsed laser deposition: characterization and application to hydrogen sensing. Appl Phys A 91:487
36. Fasaki I, Kandyla M, Tsoutsouva MG, Kompitsas M (2013) Optimized hydrogen sensing properties of nanocomposite NiO:Au thin films grown by dual pulsed laser deposition. Sens Actuators B 176:103
37. Williams DE (1999) Semiconducting oxides as gas-sensitive resistors. Sens Actuators B 57:1
38. Shankar P, Bosco J, Rayappan B (2015) Gas sensing mechanism of metal oxides: The role of ambient atmosphere, type of semiconductor and gases a review. Sci Lett J 4:126
39. Barsan N, Weimar U (2001) Conduction model of metal oxide gas sensors. J Electroceramics 7:143

40. Liu C, Kuang Q, Xie Z, Zheng L (2015) The effect of noble metal (Au, Pd and Pt) nanoparticles on the gas sensing performance of SnO_2-based sensors: a case study on the {221} high-index faceted SnO_2 octahedra. Cryst Eng Commun 17:6308
41. Müller SA, Degler D, Feldmann C, Türk M, Moos R, Fink K, Studt F, Gerthsen D, Bârsan N, Grunwaldt J-D (2018) Exploiting synergies in catalysis and gas sensing using noble metal-loaded oxide composites. Chem Cat Chem 10:864
42. Kolmakov A, Klenov DO, Lilach Y, Stemmer S, Moskovits M (2005) Enhanced gas sensing by individual SnO_2 nanowires and nanobelts functionalized with Pd catalyst particles. Nano Lett 5:667
43. Tsu K, Boudart M (1961) Recombination of atoms at the surface of thermocouple probes. Can J Chem 39:1239
44. Kandyla M, Chatzimanolis-Moustakas C, Koumoulos EP, Charitidis C, Kompitsas M (2014) Nanocomposite NiO:Au hydrogen sensors with high sensitivity and low operating temperature. Mater Res Bull 49:552
45. Morrison SR (1987) Selectivity in semiconductor gas sensors. Sens Actuators 12:425